On metrics to assess road bicycle dynamic comfort during impacts

Jean-Marc Drouet[1] · *Derek Covill*[2] · *Marianne Leroux*[1] · *Simon Richard*[1]

[1] VÉLUS Laboratory, Mechanical Engineering Department,
Université de Sherbrooke, 2500 boulevard de l'Université,
Sherbrooke, QC J1K 2R1, Canada

[2] School of Computing, Engineering and Mathematics,
University of Brighton, Cockcroft Building, Lewes Road, Brighton, England, BN1 6EF.

Citation: Drouet, J.M., Covill, D., Leroux, M. and Richard, S., 2022. On metrics to assess road bicycle dynamic comfort during impacts. *Sports Engineering*, 25(1), pp.1-15.

Abstract

A road bicycle's dynamic comfort (RBDC) relates to its capacity to filter vibration generated by the road surface. Typically, four quantities have been used to assess RBDC, acceleration, force, power and energy, however little has been done to compare the effectiveness of these in distinguishing between impact events. The aim of this study, was to assess the ability of these four quantities when measured at a cyclist's hands, to discriminate between small changes in the level of an impact load applied at the front wheel of a road bicycle. With a rider seated on a bicycle, acceleration and force time signals were recorded at the left and right hands using instrumented brake hoods during a series of impacts at the front wheel on a bicycle treadmill. Six derived parameters of the acceleration, force and power time signals were considered: discrete values: maximum, peak; mean values: root mean square, root mean quad; ratio values: crest factor, shock content quotient. Integral values were used for the energy. A range of criteria were developed to assess the performance of these parameters and whether they should be recommended as RBDC metrics for impact events. The criteria were related to three characteristics: the consistency of the measurements, the parameter's statistical discrimination power, and how well changes in the parameter matched corresponding changes in impact level. The energy and root mean square value of power were found to be the top performers and are recommended as RBDC metrics for impact events. All acceleration-based parameters are not recommended. The remaining parameters demonstrated mixed results.

Keywords: road bicycle, dynamic comfort, comfort metrics, vibration, impact loads, acceleration, force, power, energy.

1 Introduction

A road bicycle's dynamic comfort (RBDC) relates to its capacity to filter vibration generated by the road surface. It has become a key characteristic for cyclists in the process of selecting a bicycle and it is an important design issue for bicycle manufacturers [1]. In general terms, higher levels of dynamic comfort are associated with transmitting less road-induced vibration to the cyclist's hands and buttocks, but not the feet since the vibrations transmitted there do not influence comfort evaluations [2]. In recent years, a number of studies have been undertaken relating to the transmission of road-induced vibration to the cyclist. These studies focused mostly on: (1) the development of transducers to measure the forces and power transmitted at cyclist's hands and buttocks [3-6]; (2) test rigs, test protocols and measurement techniques [7-13]; (3) vibration transmissibility of bicycles, bicycle components, and cycling apparel [14-19]; (4) assessments of road surfaces [20-24]; (5) cyclists' sensory perception [2,25-27].

From a bicycle engineering standpoint, relevant quantities must be measured when assessing RBDC. Furthermore, rigorous test protocols must be implemented when taking measurements of the vibration transmitted to a cyclist [9]. Typically, four quantities have been used: acceleration [1-3,7-10,12-17,20-24,27], force [1,9,10,17,19], power [1,3,10,11,17,18,27] and energy [18,25,26]. These quantities are measured at or as close as possible to the cyclist's hands or buttocks to relate to what is experienced by the cyclist. Acceleration, which is the easiest to measure, is the most common quantity used in cycling and other fields of human vibration research (e.g. occupational health and safety). It is also used in standards that relate to shock and vibration transmitted to the hand-arm system (e.g. ISO/TS 15694:2004 [28]). Hardware in the form of accelerometers (including those embedded in smartphones) are readily available, relatively inexpensive and typically straightforward to use [13,21,24]. Force measurement is technically more difficult than acceleration measurement since it generally requires the development, fabrication and calibration of custom transducers [3-6]. It has been shown experimentally that both acceleration and force measurements are influenced considerably by the cyclist's natural position and sway, and as the forces at a cyclist's hands and buttocks increase, the acceleration tends to decrease [10]. In this context, the mechanical power and energy transmitted to these contact points have been used in several studies in an attempt to find an alternative quantity that is less sensitive to the cyclist's posture on the bicycle [1,3,10,11,17,18,27].

When comparing RBDC for two levels of a factor (e.g. road A vs road B, bike A vs bike B, component A vs component B) that vary widely in the resulting amount of vibration transmitted to the cyclist (e.g. smooth asphalt road vs cobblestone road), one expects that all of the four quantities listed above will be significantly different between the two levels. It is also expected that the cyclist be able to clearly perceive a difference between the two levels. However, the ability of these quantities to distinguish between more subtly different levels of this factor remains unknown. As a case in point for what we consider to be an appropriate differentiating benchmark for these quantities, it has been shown, in a bicycle perceptual study involving 10 participants, that they were able to differentiate between riding over dowels that varied in diameter by only 2.5 % [26].

With this in mind, the aim of this study was to assess the ability of the four quantities mentioned above (i.e. acceleration, force, power and energy) to discriminate between small changes in the level of an impact load applied at the front wheel of a road bicycle when measured at a cyclist's hands. The changes in level considered were in the vicinity of the perceptual threshold of cyclists for similar test conditions as determined previously [26]. Thereby, the corresponding changes in the quantities measured here relate directly to what can barely be perceived by cyclists, and since there is no agreement on which quantity is the most appropriate RBDC metric, this study will provide key findings for future research related to RBDC and more broadly in other fields of human vibration research.

2 Method

2.1 Laboratory set-up

All the tests described in this paper were carried out using a custom-made bicycle treadmill (Fig. 1) [25]. The treadmill platform was 76 cm wide by 196 cm long which allowed ample freedom of movement for cycling. The rear wheel was placed on a raiser board (Fig. 1 – item 5) and was thus not touching the treadmill belt (Fig. 1 – item 4). A repetitive and controlled impact load excitation was provided using an aluminium dowel (Fig. 1 – item 2) attached to the surface of the treadmill belt and was therefore applied only to the front wheel. The dowel attachment system was made up of a pair of sprung clips spaced 15 cm apart and these were glued to the treadmill belt. Bungee cables (Fig. 1 – item 3) were wrapped around the seat tube and attached to a fixed structure on each side of the treadmill in order to keep the bicycle and cyclist vertically stable. These cables were sufficiently compliant in the vertical direction to ensure that the bicycle's dynamics was not affected in that direction. A single carbon fiber road bicycle was used for all the tests (Cervélo R3 – size: 56 cm; Fulcrum 7 wheels – size: 700C; Vittoria Rubino Pro tires – width: 23 mm, pressure: 8 bars).

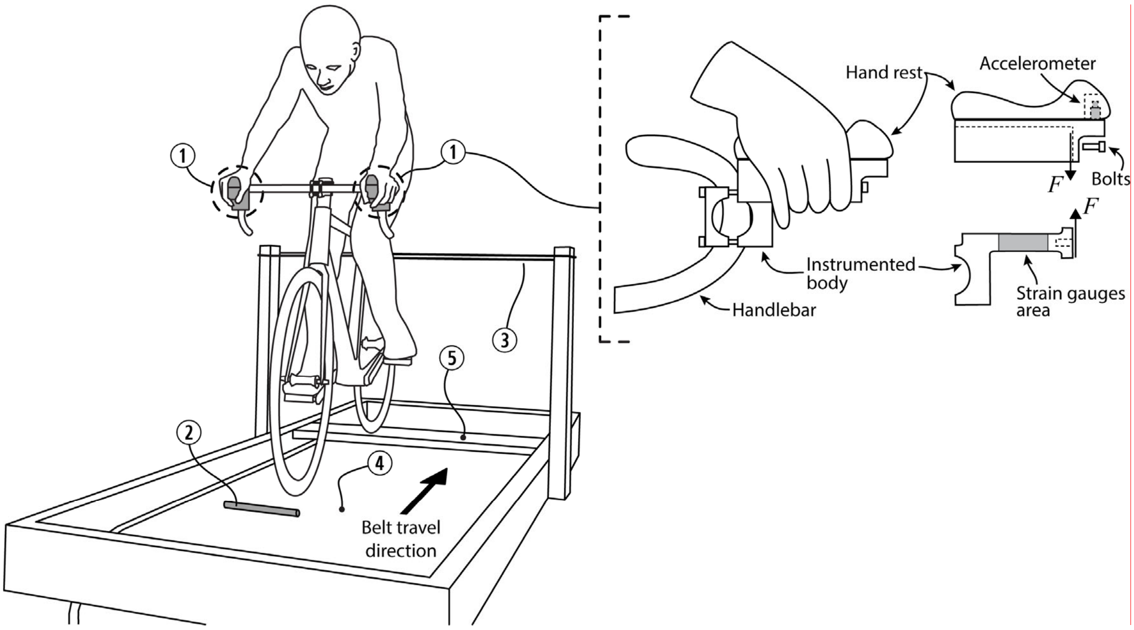

Fig. 1 Set-up for impact testing on bicycle treadmill. 1-instrumented brake hoods [1,4]; 2-aluminium dowel; 3-bungee cables; 4- treadmill belt; 5-rear wheel raiserboard

Strain gauge instrumented brake hoods [1,4] (Fig. 1 – item 1) equipped with an uniaxial accelerometer (model 352C68, PCB Piezotronics, Inc., USA – measurement range: ±50 g peak, frequency range: 0.5 to 10,000 Hz, sensitivity: 100 mV/g) were positioned under each hand to measure vertical force and vertical acceleration transmitted to the cyclist's hands. The strain gauges were arranged in a full Wheatstone bridge such that bridge signals were theoretically only sensitive to the vertical force. Calibration was performed by applying known force and moment loads to measure the direct sensitivity of the vertical force and cross-sensitivities. For the vertical forces measured, the maximum total root mean square error was within 2 % FS (Full Scale) and the non-linearity within 0.1 % FS. A 24-bit acquisition system (SCADAS model SCR01-08B, LMS International NV, Belgium) was used to collect force and acceleration signals at a sampling frequency of 8192 Hz, and Test.Lab software (LMS International NV, Belgium) and MATLAB software (The MathWorks, Inc., USA) were used for data processing.

2.2 Tests set-up

An experienced male cyclist (age: 48 years old; height: 180 cm; mass: 78 kg) was seated on the bicycle during the measurements and the bicycle was adjusted to achieve a comfortable body position for the cyclist. Following the recommendations given in [9] to reduce variability in positioning the cyclist when taking measurements on a bicycle, the cyclist posture was controlled as follows:

- The cyclist kept a natural constant position on the bicycle whilst placing his bare hands on the instrumented brake hoods and applying no grip force to them;
- The bicycle cranks were fixed in a horizontal position with the right crank at the front (no pedalling);
- The cyclist remained seated at all times.

The treadmill speed was set to 15 km/h which was deemed high enough to provide realistic impact conditions (when compared to what is experienced on the road), yet low enough to provide a sufficient amount of time for the cyclist to stabilise between impacts. The method used in this study to carry out measurements on the cyclist was approved by the ethics committee of the Université de Sherbrooke and the cyclist gave informed written consent to participate in the study.

A total of three aluminium dowels were used in this study and provided the impact levels needed to assess the ability of the quantities to distinguish between the dowel sizes. They were taken from the set of dowels used previously to assess the cyclists' perceptual threshold [26]. Their diameters (Table 1) were selected to achieve 0.2 mm, 0.4 mm and 0.6 mm differences in diameter between dowel pairs (using dowels 2-3, 1-2, and 1-3 respectively). According to [26], the 0.4 mm difference corresponds to the perceptual threshold of cyclists, and the 0.2 mm and 0.6 mm differences are therefore respectively below and above the perceptual threshold.

Three runs of 25 impacts per dowel were carried out. Data from the first 5 impacts of each run were discarded since during these impacts the cyclist was getting settled. A permutated block randomization approach was used to create a 60 impacts data set for each dowel. The cyclist dismounted the bicycle completely after each run. All the runs were carried out in a single session that lasted 60 minutes.

Table 1 Designation and diameter dimension of the dowels

Dowel designation	Dowel diameter (mm)
1	$d_1 = 15.1$
2	$d_2 = 15.5$
3	$d_3 = 15.7$

2.3 Measurements at the cyclist's hands

The four quantities considered in this study were: the vertical acceleration, vertical force, power and energy transmitted to the cyclist's hands. Basic quantities of acceleration, a, and force, F, were directly measured using the instrumented brake hoods. The DC component of the force signal (also called the static force or push force) was removed since it is not related to the impact excitation. The instantaneous power transmitted to the cyclist's hands, P, was calculated using (1) where v is the vertical speed (obtained by integrating the acceleration time signal).

$$P(t) = F(t)v(t) \tag{1}$$

The energy transmitted to the cyclist's hands, E, for each impact was calculated over the duration of a given impact using (2).

$$E = \int P(t)dt \tag{2}$$

Acceleration and force time signals were used in two separate ways: (1) unweighted and (2) weighted using flat_h weighting as outlined in ISO/TS 15694:2004 [28]. Flat_h was used here since it is the standard weighting for single shocks transmitted from hand-held and hand-guided machines to hand-arm systems [28]. Even though flat_h weighting is applied to acceleration only in ISO/TS 15694:2004, it was also applied in this study to the force time signal for completeness. Power and energy were calculated for both cases i.e. using unweighted a/F time signals and using flat_h-weighted a/F time signals.

For each impact, six derived parameters of the acceleration, force and power time signals were considered: the maximum value, the peak value (PV), the root mean square (RMS) value, as well as root mean quad (RMQ) value where the influence of the higher magnitudes is stronger than with the RMS value, and both the crest factor (CF) and shock content quotient (SC) values which describe the impulsiveness of the signal [28]. These parameter values can be categorised as discrete (i.e. maximum value and PV), mean (i.e. RMS and RMQ values) and ratios (i.e. CF and SC values). They were all evaluated at the left and right hands separately using (3) to (8) respectively, where w represents the acceleration, force or power, and N is the number of sampled values of w over the duration of a given impact. Even though CF and SC are applied to acceleration only in ISO/TS 15694:2004, we have also calculated CF and SC for force and power for completeness. The energy (an integral value) was evaluated at the left and right hands separately. The total energy transmitted to the cyclist's hands was also calculated by adding the energy transmitted to both hands.

$$w_{\max} = \max\{w_i\} \qquad \text{with } i = 1, 2, \ldots, N \tag{3}$$

$$w_{\mathrm{PV}} = \max\{|w_i|\} \qquad \text{with } i = 1, 2, \ldots, N \tag{4}$$

$$w_{\mathrm{RMS}} = \left[\frac{1}{N}\sum_{i=1}^{N} w_i^2\right]^{\frac{1}{2}} \tag{5}$$

$$w_{\mathrm{RMQ}} = \left[\frac{1}{N}\sum_{i=1}^{N} w_i^4\right]^{\frac{1}{4}} \tag{6}$$

$$CF = \frac{w_{\mathrm{PV}}}{w_{\mathrm{RMS}}} \tag{7}$$

$$SC = \frac{w_{\mathrm{RMQ}}}{w_{\mathrm{RMS}}} \tag{8}$$

Typical plots of the time signal of the instantaneous power transmitted at a cyclist's hand are presented in Fig. 2. With the treadmill speed set to 15 km/h, two consecutive impacts were separated by a constant time interval Δt_{i} = 1.31 s, so the recording duration for a run of 25 impacts lasted approximately 35 s. To calculate the energy integral as well as the RMS, RMQ, CF and SC values for a given impact, it was necessary to estimate a time window within which the impact occurred. Furthermore, it was also required that this time window be of the same duration and relative location for all the impacts in this study in order to have a common basis for comparison of parameters.

As shown in Fig. 2, as a result of the tightly controlled nature of the test conditions, the overall shape of the power time signal was similar for each impact and was characterized by the presence of a distinctive high peak. Since this peak was easy to locate, it was chosen as the time window reference position. The time window for each impact (shown between dotted lines in Fig. 2) was determined by looking at the power time signal, and judging the beginning and end of the impact on either side of the distinctive power peak. It was determined that an impact began as the power started to be transmitted to the cyclist's hands (easily identifiable by a steep rise in the power time signal) and ended when the transmitted power dropped (and remained) below 0.5 W (i.e. less than 1 % of the peak power value in the worst case scenario). The time window was then calculated by adding together the time windows before and after this peak (Δt_1 = 0.07 s and Δt_2 = 0.16 s respectively). The time window duration encompasses every impact in this study.

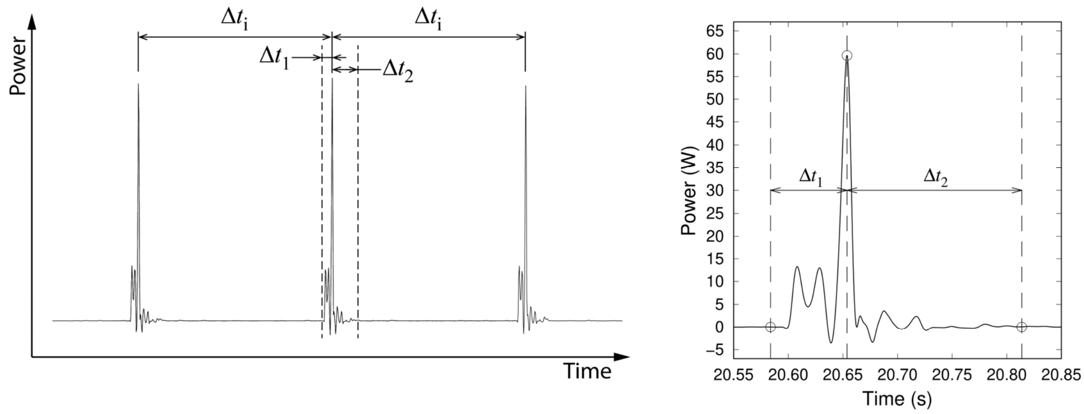

(a) Typical plot showing a series of impact events. **(b)** Typical plot showing a single impact event.

Fig. 2 Typical plots of the time signal of instantaneous power transmitted at a cyclist's hand. The time window for an impact is indicated between the dashed lines and this was comprised of the period before (Δt_1 = 0.07 s) and (

Δt_2 = 0.16 s) the distinctive power peak. The period between impacts is indicated here between sequential power peaks which served as identifiable reference points to locate time windows (Δt_i = 1.31 s).

This method section provided a description of both the laboratory set-up and test set-up and included details of how the measurements were collected and processed. A description of the data analysis methods used is provided in the following section alongside the results in order to explain these methods with the aid of actual data to help with the explanation.

3 Results and data analysis

Data was analysed using the following three approaches: (1) a comparison of the means; (2) a comparison of the ratio of the changes in each parameter as they relate to ratio of the changes in dowel size; (3) an evaluation of the correlation between the parameters at the left and right hands. The bootstrap method [29,30] and confidence intervals (CIs) [31,32], based on the 60 impacts data set available for each dowel, were used for the statistical analyses carried out in this study. The bootstrap method is based on the resampling with replacement of the original data sets. This technique allows us to resample the original data sets in order to assess the statistical power of a given parameter as explained below.

3.1 Comparison of the means

The bootstrap means and 95 % CIs for acceleration-based parameters (Fig. 3), force-based parameters (Fig. 4), and power-based parameters and energy (Fig. 5) were derived using $B = 10^6$ bootstrap samples of size $n = 60$ generated from the original data sets according to [29]. In all cases, results for the maximum value and peak value (PV) were identical, and are presented together herein.

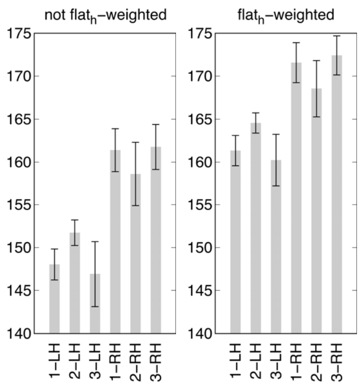

(a) $a_{\max}$ and a_{PV} (m/s^2)

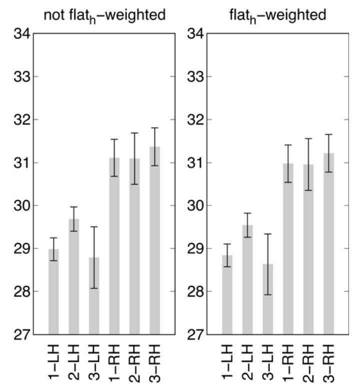

(b) a_{RMS} (m/s^2)

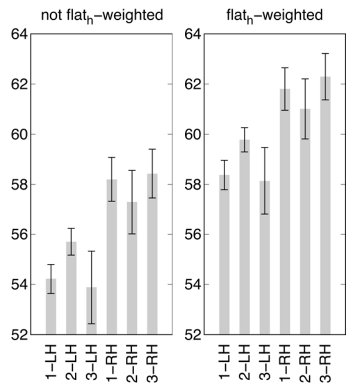

(c) a_{RMQ} (m/s^2)

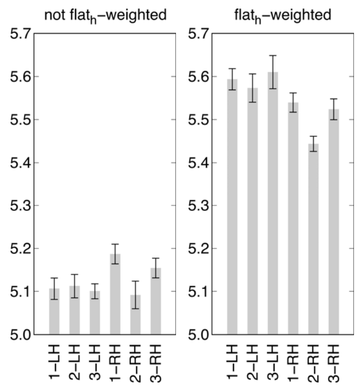

(d) *CF* for acceleration

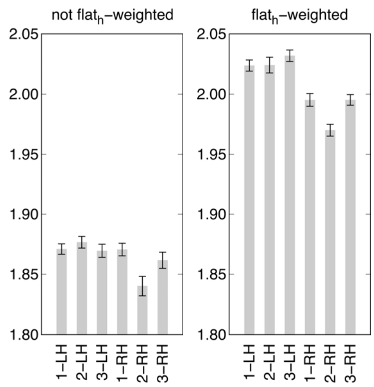

(e) *SC* for acceleration

Fig. 3 Bootstrap mean and 95 % confidence interval (n = 60; $B = 10^6$) for all acceleration-based parameters for each of the three dowels (1-3). Not flat$_h$-weighted and flat$_h$-weighted data is presented for both the left-hand (LH) and right-hand (RH). Note: PV: peak value; RMS: root mean square; RMQ: root mean quad; CF: crest factor; SC: shock content quotient.

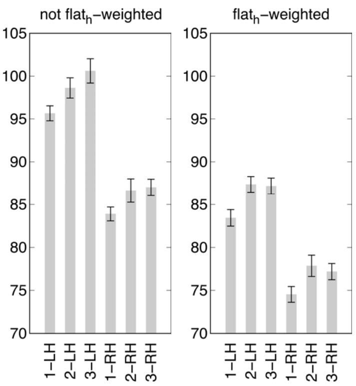

(a) F_{max} and F_{PV} (N)

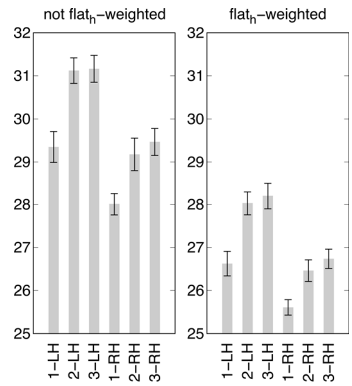

(b) F_{RMS} (N)

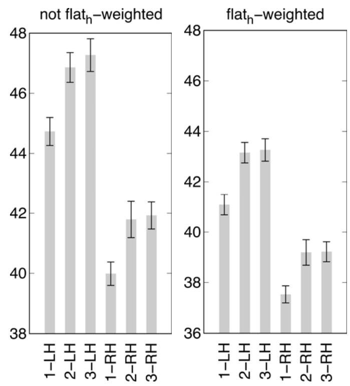

(c) F_{RMQ} (N)

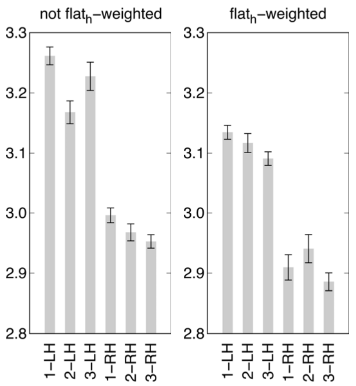

(d) *CF* for force

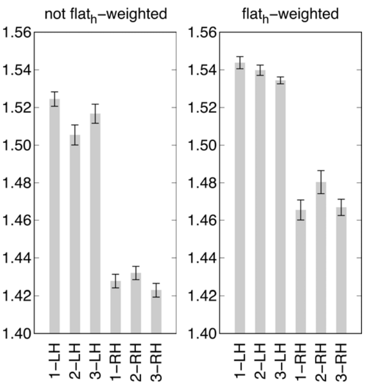

(e) *SC* for force

Fig. 4 Bootstrap mean and 95 % confidence interval (n = 60; $B = 10^6$) for all force-based parameters for each of the three dowels (1-3). Not flat$_h$-weighted and flat$_h$-weighted data is presented for both the left-hand (LH) and right-hand (RH). Note: PV: peak value; RMS: root mean square; RMQ: root mean quad; CF: crest factor; SC: shock content quotient.

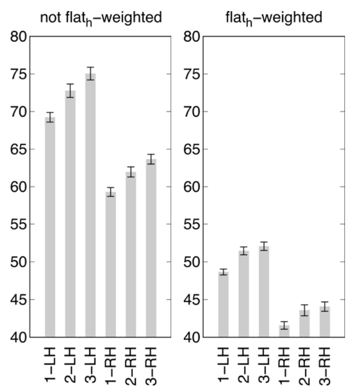

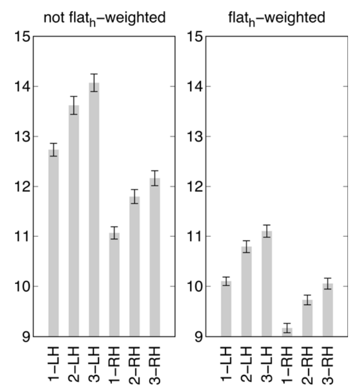

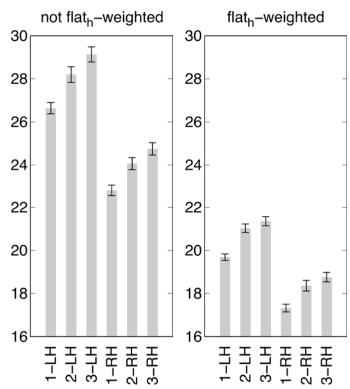

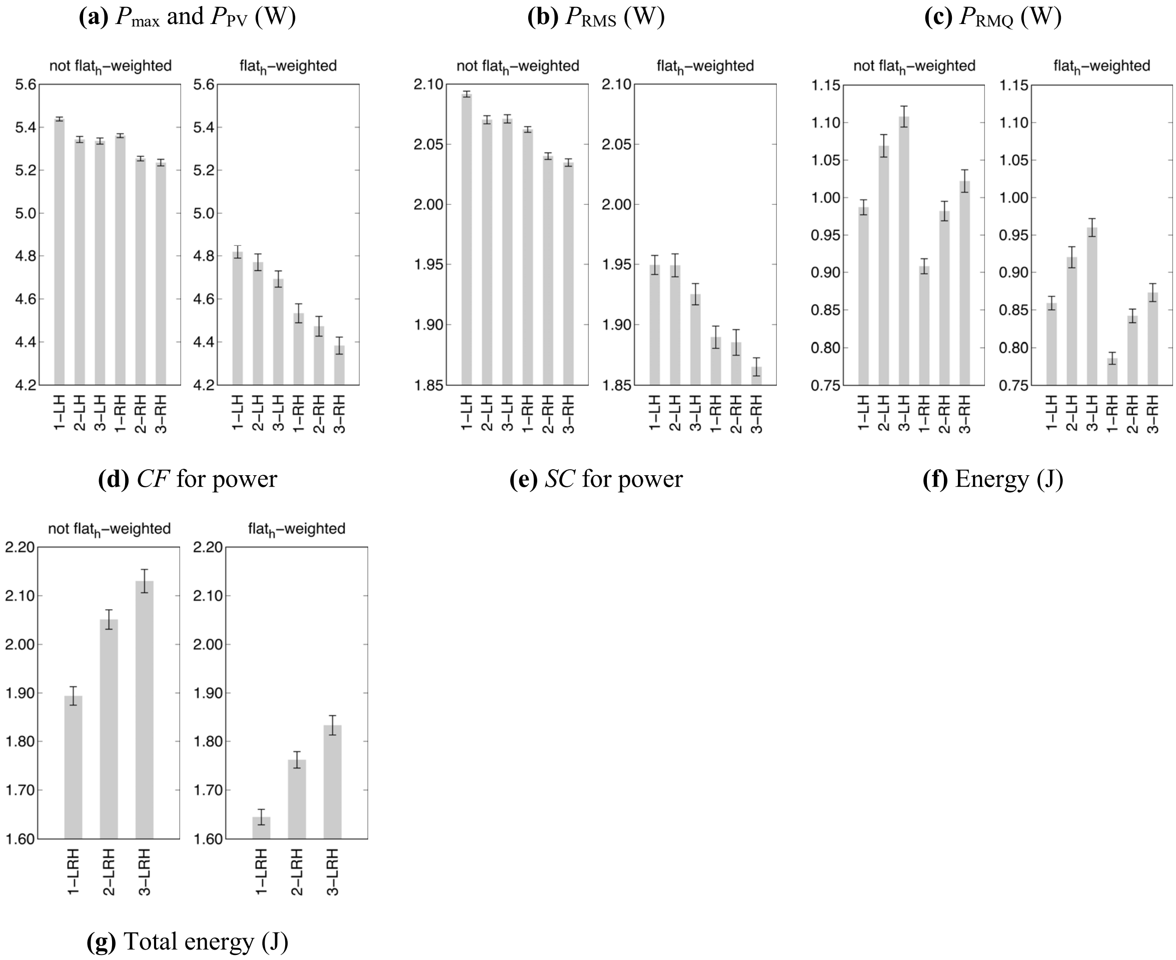

Fig. 5 Bootstrap mean and 95 % confidence interval ($n = 60$; $B = 10^6$) for all power-based parameters, energy and total energy for each of the three dowels (1-3). Not flat$_h$-weighted and flat$_h$-weighted data is presented for both the left-hand (LH), right-hand (RH), and left and right hands combined (LRH; total energy only). Note: PV: peak value; RMS: root mean square; RMQ: root mean quad; CF: crest factor; SC: shock content quotient.

From the experimenter standpoint, keeping the excitation-induced strain as low as possible for RBDC study participants is paramount. When using impact load, knowledge of the minimum sample size (i.e. minimum number of impacts) required to achieve statistical differentiation between levels of a factor helps to better fulfill this objective. Therefore, in this study, the statistical discrimination power of a given parameter was assessed using the minimum sample size value: the lower this value, the higher the discrimination power of the parameter. To this end, a two-step approach based on [31,32] was used. Firstly, 90 %, 95 % and 99 % bootstrap CIs (unadjusted for multiple comparisons) with sample size ranging from 2 to 60 and $B = 10^6$ were constructed for the difference of the means, $\overline{p}_i^* - \overline{p}_j^*$, for each parameter p for dowels i and j ($i, j = 1, 2, 3$; $i < j$). Secondly, the minimum sample size required for $\overline{p}_i^* - \overline{p}_j^* = 0$ to fall outside of the CIs was determined.

Typical results are presented in Fig. 6. In Fig. 6a, the CIs for P_{max} (dowels 2 and 3; right hand; flat$_h$-weighted) are plotted as a function of the bootstrap sample size. Since the 90 % CI encompasses the zero difference of means line (i.e. $\overline{P}_{max,2}^* - \overline{P}_{max,3}^* = 0$) for any sample size, flat$_h$-weighted P_{max} doesn't allow for the differentiation of dowels 2 and 3 at the right hand. Figure 6b shows that a minimum sample size of 13, 19 and 32 for the 90 %, 95 % and 99 % CIs respectively would be required for flat$_h$-weighted a_{RMS} to differentiate between dowels 1 and 2 at the left hand.

Figure 6c shows that flat$_h$-weighted total energy (i.e. left and right hands combined) allows for the differentiation of dowels 1 and 3 at or above sample sizes of only 2 (regardless of which CI is used), demonstrating a clear ability to statistically distinguish between dowels. Table 2 presents the minimum sample size, for each parameter and CI.

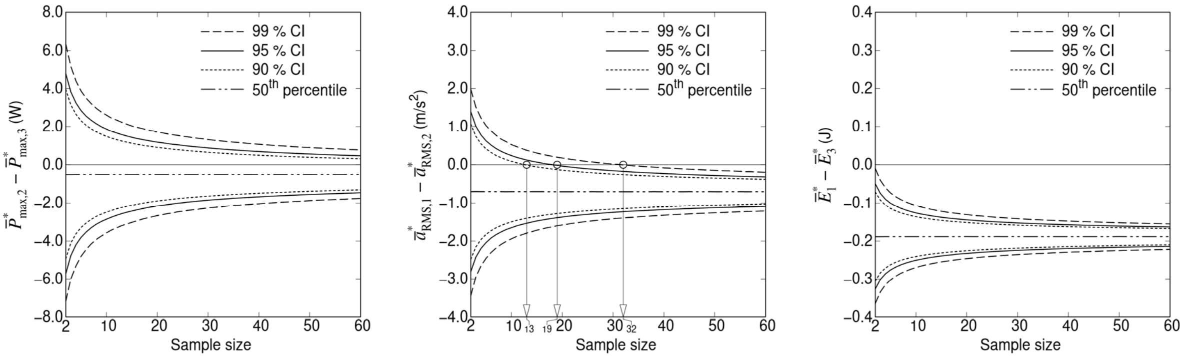

(a) P_{max} or P_{PV} (RH; dowels 2 and 3; flat$_h$-weighted)

(b) a_{RMS} (LH; dowels 1 and 2; flat$_h$-weighted)

(c) Energy (LRH; dowels 1 and 3; flat$_h$-weighted)

Fig. 6 Typical results assessing the ability of the parameters to distinguish between dowel sizes using 90 %, 95 % and 99 % bootstrap CIs (sample size ranging from 2 to 60; $B = 10^6$) for the difference of the means (i.e. $\overline{p}_i^* - \overline{p}_j^*$; parameter p; dowels i and j with $i, j = 1, 2, 3$ and $i < j$): (a) flat$_h$-weighted P_{max} doesn't allow for the differentiation of dowels 2 and 3 at the right hand; (b) a minimum sample size of 13, 19 and 32 for the 90 %, 95 % and 99 % CIs respectively would be required for flat$_h$-weighted a_{RMS} to differentiate between dowels 1 and 2 at the left hand; (c) flat$_h$-weighted total energy allows for the differentiation of dowels 1 and 3 at or above sample sizes of only 2 (regardless of which CI is used). Note: RMS: root mean square; LH: left hand; RH: right hand; LRH: left and right hands combined.

Table 2 Minimum sample size, *n*, required to distinguish between dowels for each parameter for the 90 %/95 %/99 % CIs. Data is presented for both *without flat$_h$* **;** *with flat$_h$* weighting.

Dowel pair	2-3		1-2		1-3	
Δ*d* (mm)	0.2		0.4		0.6	
Side	LH	RH	LH	RH	LH	RH
acceleration						
max, PV	31/44/●* ; 25/35/●*	● ; 45/●/●	17/24/41 ; 18/26/44	●* ; ●*	●* ; ●*	● ; ●
RMS	33/47/●* ; 32/45/●*	● ; ●	13/18/31 ; 13/19/32	●* ; ●*	●* ; ●*	● ; ●
RMQ	32/46/●* ; 33/48/●*	● ; 56/●/●	12/17/29 ; 13/18/31	●* ; ●*	●* ; ●*	● ; ●
CF	●* ; ●	17/23/39 ; 6/9/14	● ; ●*	8/10/18* ; 4/6/10*	●* ; ●	44/●/●* ; ●*
SC	44/●/●* ; 48/●/●	10/14/24 ; 3/5/7	54/●/● ; ●	5/6/10* ; 4/5/9*	●* ; 30/42/●	40/57/●* ; ●
force						
max, PV	● ; ●*	● ; ●*	11/16/28;6/8/13	14/21/35;10/13/23	5/8/13;6/9/15	8/10/18;11/15/27
RMS	● ; ●	● ; ●	4/5/8 ; 4/6/9	7/9/15 ; 6/8/13	4/5/8 ; 4/5/8	4/5/8 ; 3/4/7
RMQ	● ; ●	● ; ●	5/7/12 ; 4/5/9	7/10/16 ; 6/8/13	4/5/9 ; 4/5/9	5/6/10 ; 5/6/10
CF	12/16/27 ; 23/33/54*	59/●/●* ; ●*	3/4/7* ; 53/●/●*	19/26/46* ; 45/●/●	27/38/●* ; 6/9/15*	7/9/15* ; 50/●/●*
SC	19/26/44 ; 16/23/39*	13/18/31* ; 14/19/32*	5/7/12* ; 48/●/●*	● ; 13/19/33	28/39/●* ; 7/10/16*	47/●/●* ; ●
power						
max, PV	13/18/29 ; ●	14/19/33 ; ●	5/6/10 ; 3/4/6	5/7/12 ; 9/12/21	2/2/4 ; 2/3/4	2/3/5 ; 5/7/11
RMS	14/19/32 ; 13/19/31	14/20/34 ; 9/13/22	3/4/6 ; 2/3/5	3/4/7 ; 3/4/6	2/2/3 ; 2/2/3	2/2/4 ; 2/2/3
RMQ	13/18/29 ; 32/45/●	15/21/36 ; 30/42/●	4/5/9 ; 2/3/4	4/6/9 ; 4/6/9	2/2/3 ; 2/2/3	2/3/4 ; 2/3/4
CF	●* ; 21/28/48*	42/58/●* ; 20/28/47*	2/2/4* ; 43/●/●*	2/2/2* ; ●*	2/2/3* ; 6/9/15*	2/2/2* ; 7/10/17*
SC	● ; 13/18/28*	26/37/●* ; 18/25/42*	2/3/5* ; ●*	2/2/3* ; ●*	2/3/5* ; 11/15/24*	2/2/2* ; 10/15/24*
energy						
	12/17/28 ; 10/13/22	10/15/25 ; 10/13/23	2/3/5 ; 3/4/7	3/3/5 ; 2/3/5	2/2/2 ; 2/2/3	2/2/3 ; 2/2/3
	LRH: 8/10/18 ; 6/8/14		LRH: 2/2/4 ; 2/3/4		LRH: 2/2/2 ; 2/2/2	

Note 1: PV: peak value; RMS: root mean square; RMQ: root mean quad; CF: crest factor; SC: shock content quotient; LH: left hand; RH: right hand; LRH: left and right hands combined; *: 50th percentile value is greater than zero (i.e. where a larger dowel produced a lower parameter value).
Note 2: ●: zero difference of means not outside of CI for any sample size. Where only a single ● is displayed, the zero difference of means is not outside of the 90 % CI for any sample size.

3.2 Changes in parameters in relation to the changes in dowel size

The relative changes in each parameter were compared to the corresponding changes in dowel size in order to establish if there was a relationship between them. The benchmark used was the diameter difference ratio (DDR), δ^{dowel}, which compared the relative changes in dowel diameter and was calculated using (9a-c).

$$\delta_{\text{a}}^{\text{dowel}} = \frac{d_3 - d_1}{d_2 - d_1} \tag{9a}$$

$$\delta_{\text{b}}^{\text{dowel}} = \frac{d_2 - d_1}{d_3 - d_2} \tag{9b}$$

$$\delta_{\text{c}}^{\text{dowel}} = \frac{d_3 - d_1}{d_3 - d_2} \tag{9c}$$

Given the values of the dowel diameters (Table 1), the values of the DDRs $\delta_{\text{a}}^{\text{dowel}}$, $\delta_{\text{b}}^{\text{dowel}}$ and $\delta_{\text{c}}^{\text{dowel}}$ were 1.5, 2 and 3 respectively. As such, these three values were compared to all equivalent parameter difference ratios (PDRs), δ^{param}, which were determined using (10a-c).

$$\delta_{\text{a}}^{\text{param}} = \frac{M_3 - M_1}{M_2 - M_1} \tag{10a}$$

$$\delta_{\text{b}}^{\text{param}} = \frac{M_2 - M_1}{M_3 - M_2} \tag{10b}$$

$$\delta_{\mathrm{c}}^{\mathrm{param}} = \frac{M_3 - M_1}{M_3 - M_2} \tag{10c}$$

where M_i is the bootstrap mean value (n = 60, B = 10^6) of a given parameter associated with dowel i (i = 1, 2, 3). The PDRs for all parameters are shown in Table 3.

Table 3 Values of the parameter difference ratios (PDRs), $\delta_{\mathrm{a}}^{\mathrm{param}} / \delta_{\mathrm{b}}^{\mathrm{param}} / \delta_{\mathrm{c}}^{\mathrm{param}}$, for all bootstrap mean values (n = 60; B = 10^6) to be compared with dowel difference ratios (DDRs) 1.5/2/3.

	not $\mathrm{flat_h}$-weighted		$\mathrm{flat_h}$-weighted	
Side	LH	RH	LH	RH
acceleration				
max, PV	-0.31/-0.77/0.23	-0.11/-0.90/0.10	-0.34/-0.75/0.25	-0.27/-0.79/0.22
RMS	-0.27/-0.79/0.22	-13/-0.069/0.93	-0.29/-0.77/0.23	-12/-0.075/0.93
RMQ	-0.23/-0.81/0.19	-0.25/-0.80/0.20	-0.17/-0.85/0.15	-0.62/-0.62/0.38
CF	-1.0/-0.50/0.50	0.34/-1.5/-0.53	-0.80/-0.56/0.45	0.16/-1.2/-0.19
SC	-0.25/-0.80/0.20	0.29/-1.42/-0.42	24/0.044/1.0	-0.0033/-1.0/0.0033
force				
max, PV	1.7/1.5/2.5	1.1/7.5/8.5	0.95/-21/-20	0.79/-4.8/-3.8
RMS	1.0/43/44	1.2/4.0/5.0	1.1/8.3/9.3	1.3/3.1/4.1
RMQ	1.2/5.2/6.2	1.1/14/15	1.1/19/20	1.0/59/60
CF	0.36/-1.57/0.57	1.5/1.9/2.9	2.5/0.68/1.7	-0.76/-0.57/0.43
SC	0.41/-1.7/-0.7	-1.1/-0.47/0.53	2.4/0.74/1.7	0.10/-1.1/-0.10
power				
max, PV	1.6/1.6/2.6	1.6/1.6/2.6	1.2/4.6/5.6	1.2/4.1/5.1
RMS	1.5/2.0/3.0	1.5/2.0/3.0	1.4/2.2/3.2	1.6/1.8/2.8
RMQ	1.6/1.7/2.7	1.6/1.8/2.8	1.2/4.1/5.1	1.4/2.6/3.6
CF	1.1/14/15	1.2/5.7/6.7	2.6/0.62/1.6	2.5/0.67/1.7
SC	0.97/-29/-28	1.2/4.1/5.1	75/0.013/1.0	5.7/0.21/1.2
energy				
	1.5/2.1/3.1	1.5/1.9/2.9	1.7/1.5/2.5	1.5/1.8/2.8
	LRH: 1.5/2.0/3.0		LRH: 1.6/1.6/2.6	

Note: PV: peak value; RMS: root mean square; RMQ: root mean quad; CF: crest factor; SC: shock content quotient; LH: left hand; RH: right hand; LRH: left and right hands combined.

3.3 Correlation between the parameters at the left and right hands

In order to compare the amount of vibration transmitted at the left and right hands for a typical scenario, the correlation between parameters at both hands was evaluated based on the original 60 impacts data sets for each parameter (not $\mathrm{flat_h}$-weighted and $\mathrm{flat_h}$-weighted) using dowel 1. The results for $\mathrm{flat_h}$-weighted shock content quotient for power are presented in Fig. 7a, showing the highest coefficient of determination, R^2 = 0.577 indicating a high correlation [33]. Results for the other parameters showed a lower correlation between the left and right hands, with typical values in the very low to moderate range for correlation, down to a value of 0.018 for the shock content quotient for acceleration (not $\mathrm{flat_h}$-weighted). Results for $\mathrm{flat_h}$-weighted a_{RMS} and F_{RMS} are shown in Figs 7b and 7c respectively as an example to demonstrate that as the force at a cyclist's hand increases, the acceleration tends to decrease as previously noted in [10].

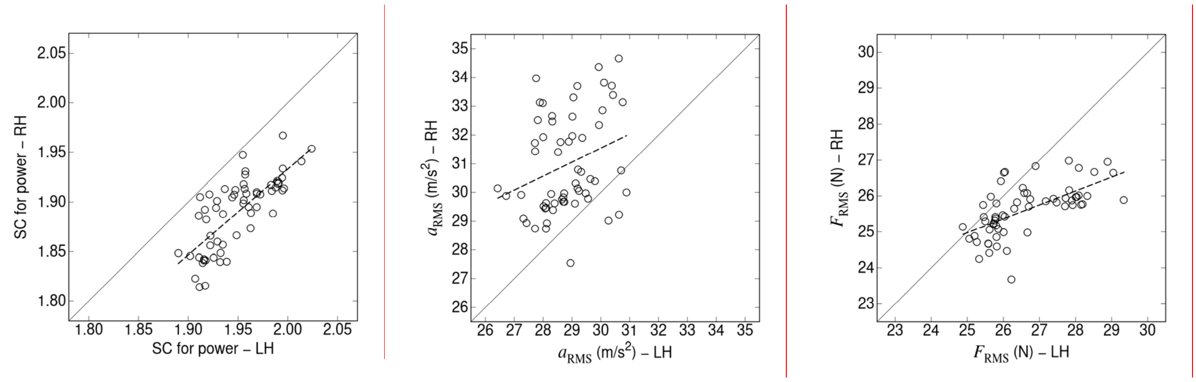

(a) **(b)** **(c)**

Fig. 7 Corresponding (a) flat$_h$-weighted *SC* for power (R^2 = 0.577), (b) flat$_h$-weighted a_{RMS} (R^2 = 0.088) and (c) flat$_h$-weighted F_{RMS} (R^2 = 0.385) for the left and right hands using dowel 1. Note: SC: shock content quotient; RMS: root mean square; LH: left hand; RH: right hand.

4 Discussion

The results presented in this paper demonstrate that there were clear differences in the parameters' abilities to differentiate between the dowels (Figs. 3-5 and Table 2). Indeed, from an RBDC perspective, it should be a requirement that a parameter should at least be capable of differentiating even the smallest change in dowel sizes used here (i.e. dowel pair 2-3), since these correspond to impact differences that were in the vicinity of the perceptual threshold of cyclists [26]. In addition, there were also clear differences in how the changes in the parameters themselves compared with the corresponding changes in dowel size (Table 3).

4.1 Criteria for RBDC metrics

With these points in mind, a range of criteria were developed to assess whether these parameters should be recommended as RBDC metrics. The criteria were related to three characteristics: (1) the *consistency* of the measurements, (2) the parameter's *discrimination power*, and (3) how well changes in the parameter matched corresponding changes in dowel size (i.e. PDRs vs DDRs). The criteria were defined as follows:

1. *Consistency criterion*, where parameters were classified by whether or not (a) increasingly different dowel pairs relate to decreasing or constant minimum sample size required to distinguish between the dowels, and (b) increases in the excitation level (i.e. impact using a larger dowel) related to always increasing or always decreasing parameter values. In order to meet the *consistency criterion*, parameters were required to satisfy both of these conditions for both hands (see Table 2).

2. *Discrimination power criterion*, where parameters were classified across two dimensions based on results presented in Table 2. Firstly, whether or not they could distinguish between the three decreasingly different dowel pairs, i.e. A: can distinguish between all three pairs, Δd = 0.2 mm (dowel pair 2-3), B: can distinguish between pairs 1-2 and 1-3, Δd = 0.4 mm (dowel pair 1-2), C: can distinguish between pair 1-3 only, Δd = 0.6 mm. Secondly, they were assessed by the minimum sample size, n, required to achieve this, i.e. 1: $n \leq 20$, 2: $20 < n \leq 40$, 3: $40 < n \leq 60$. In order to meet a certain classification for the *discrimination power criterion*, parameters were required to at least satisfy the same conditions for both hands (e.g. if the left hand is B1 and the right hand is B2, then the classification will be B2).

3. *PDR-DDR criterion* where the relative difference $\Delta\delta = 100\left|\delta^{\text{param}} - \delta^{\text{dowel}}\right| / \delta^{\text{dowel}}$ was calculated for each parameters. In order to meet the *PDR-DDR criterion*, $\Delta\delta$ should be $\leq$ 10 % for both hands.

4.2 Recommendations for RBDC metrics

Results of the evaluation of the three criteria are presented in Table 4. Based on this evaluation, the level of recommendation for the parameters to be used as RBDC metrics was established (Table 4) and is either one the following:

- **Highly recommended** (HR): The *consistency criterion* is met - and - the *discrimination power criterion* is met with A3 or better for the three CIs - and - the *PDR-DDR criterion* is met .
- **Recommended** (R): The *consistency criterion* is met - and - the *discrimination power criterion* is met with A3 or better for the three CIs - and - the *PDR-DDR criterion* is not met.
- **Recommended with limitation** (RL): Do not qualify for the levels HR and R - and - the *consistency criterion* is met - and - the *discrimination power criterion* is met with B3 or better for the three CIs - and - the *PDR-DDR criterion* is met or not. The limitation implied here is related to the *discrimination power criterion* only.
- **Not recommended** (NR): Do not qualify for the three other levels.

Table 4 Overall assessments for the parameters as RBDC metrics based on the *consistency criterion*, the *discrimination power criterion* and the *PDR-DDR criterion*. Data is presented for both *without* $flat_h$ **;** *with* $flat_h$ weighting.

	Consistency criterion	*Discrimination power criterion* for the 90 %/95 %/99 % CIs	*PDR-DDR criterion* ($\Delta\delta$)	Level of recommendation
acceleration				
max, PV	- **;** -	- **;** -	- **;** -	NR **;** NR
RMS	- **;** -	- **;** -	- **;** -	NR **;** NR
RMQ	- **;** -	- **;** -	- **;** -	NR **;** NR
CF	- **;** -	- **;** -	- **;** -	NR **;** NR
SC	- **;** -	- **;** -	- **;** -	NR **;** NR
force				
max, PV	Y **;** -	B1/B2/B2 **;** B1/B1/B2	- **;** -	RL **;** NR
RMS	Y **;** Y	B1/B1/B1 **;** B1/B1/B1	- **;** -	RL **;** RL
RMQ	Y **;** Y	B1/B1/B1 **;** B1/B1/B1	- **;** -	RL **;** RL
CF	- **;** -	A3/C2/- **;** -/-/-	- **;** -	NR **;** NR
SC	- **;** -	C3/-/- **;** A1/A2/A2	- **;** -	NR **;** NR
power				
max, PV	Y **;** Y	A1/A1/A2 **;** B1/B1/B2	- **;** -	R **;** RL
RMS	Y **;** Y	A1/A1/A2 **;** A1/A1/A2	0 % **;** 10 %	HR **;** HR
RMQ	Y **;** Y	A1/A2/A2 **;** A2/A3/B1	- **;** -	R **;** RL
CF	Y **;** -	B1/B1/B1 **;** C1/C1/C1	- **;** -	R **;** NR
SC	Y **;** -	B1/B1/B1 **;** C1/C1/C2	- **;** -	R **;** NR
energy				
LH/RH	Y **;** Y	A2/A2/A3 **;** A2/A2/A3	5 % **; -**	HR **;** R
LRH	Y **;** Y	A1/A1/A1 **;** A1/A1/A2	0 % **; -**	HR **;** R

Note 1: PV: peak value; RMS: root mean square; RMQ: root mean quad; CF: crest factor; SC: shock content quotient; LH: left hand; RH: right hand; LRH: left and right hands combined.
Note 2: Dash (-) indicates that the parameter did not meet the criteria.
Note 3: Y is indicated for the *consistency criterion* where parameters met this criterion.
Note 4: The $\Delta\delta$ value displayed for the *PDR-DDR criterion* is the higher of the two values calculated at LH or RH (i.e. worst case scenario).

The overall assessments presented in Table 4 indicate that power and energy performed convincingly better than the basic quantities of acceleration and force, in the context of this study. They also strongly suggest that the acceleration-based parameters should not be used for RBDC assessment in the case of impact events despite the fact that some of them are commonly used in the RBDC literature. Regarding force-based parameters, even though some of them are recommended with limitation, the authors believe that researchers might as well go the extra step and use power or energy. This study thus revealed that measurements of acceleration and force with their limited ability to distinguish between dowels or correlate with the DDRs, when combined to obtain power and energy, the ability to differentiate between dowels and to correlate with DDRs is vastly improved. It should be noted that, for two of the recommended parameters, *CF* and *SC* for power, the 50th percentile value for the CIs is positive, indicating that impacting a larger dowel resulted in a lower parameter value. The authors suggest however, in the context of RBDC assessment, to use recommended parameters that display intuitive trends i.e. impacting a larger dowel resulting in a higher parameter value.

As shown in Table 4, the only parameter to be highly recommended in both its unweighted and flat$_h$-weighted variants is P_{RMS}. The individual energy (left or right hands) and total energy (left and right hands combined) are highly recommended only in their unweighted variant. As a general observation of the data presented in Table 4, flat$_h$ weighting seems to be detrimental to the parameters' performance in relation with the three criteria. In the context of this study, there thus appears to be no identifiable benefit in using the flat$_h$ weighting approach. As such it could be argued that flat$_h$ weighting, which adds some computational burden for researchers, be used only when deemed absolutely required for the study at hand. In the case of the *PDR-DDR criterion*, because flat$_h$ weighting removes some of the frequency content from the original acceleration and force time signals, it could also be argued that flat$_h$-weighted parameters will be less representative of the dowels, as highlighted in Table 4 for P_{RMS} and the energy.

The observed correlation between parameters at the left and right hands, which typically varies between negligible and moderate, is believed to be due, in part, to the inherent variability of the cyclist, and also to the short period of instability after the impact. During these events, the cyclist had to steer the bike as straight as possible while keeping a constant posture on the bicycle. Despite this level of correlation, according to the definition of the three criteria, any of the highly recommended (HR), recommended (R) and recommended with limitations (RL) parameters could be measured at either the left or right hand.

4.3 Influence of the cyclist's posture

Of interest is also the consistency of the cyclist's posture during these experiments and indeed what influence the cyclist's posture has on the overall results. As stated in section 2.2, following the recommendations given in [9], the cyclist's posture was kept as constant as possible and one key element related to this is the DC force applied to the instrumented brake hoods which should also be as constant as possible. Even if it's not the aim of this study, a two-fold post-hoc analysis was carried out on the DC force. Firstly, across all impacts (n = 180), the mean and 95 % CI of the DC force were calculated for the left hand, right hand and both hands. The results of this analysis presented in Fig. 8 show a small confidence interval in each case suggesting a highly constant posture.

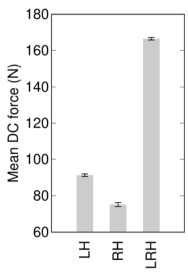

Fig. 8 DC force mean and 95 % confidence interval for all runs with all dowel sizes (n = 180). Note: LH: left hand; RH: right hand; LRH: left and right hands combined.

Secondly, we evaluated the variability in the six derived parameters that can be accounted for by variations in the DC force. To that end, we calculated the coefficient of determination between each of the parameters and the DC force as shown in Fig. 9. It can be seen that the general trend mirrors that of the recommendations outlined above in Table 4. Acceleration and force showed a moderate to high degree of variability due to the DC force, which typically accounted for over half of the variability in these parameters. On the other hand, the highly recommended parameters of P_{RMS} and the energy parameters demonstrated low to very low variability due to the DC force which typically accounted for less than a quarter of the variability. Of note also are the typically low values for crest factor (CF) and shock content quotient (SC), since these are ratios where any influence of the DC force is believed to be cancelled out, despite the fact that they are generally not recommended as RBDC metrics. An evaluation such as this can provide some indication as to why some parameters perform better than others and hence it is recommended that the influence of DC force be a topic for further study.

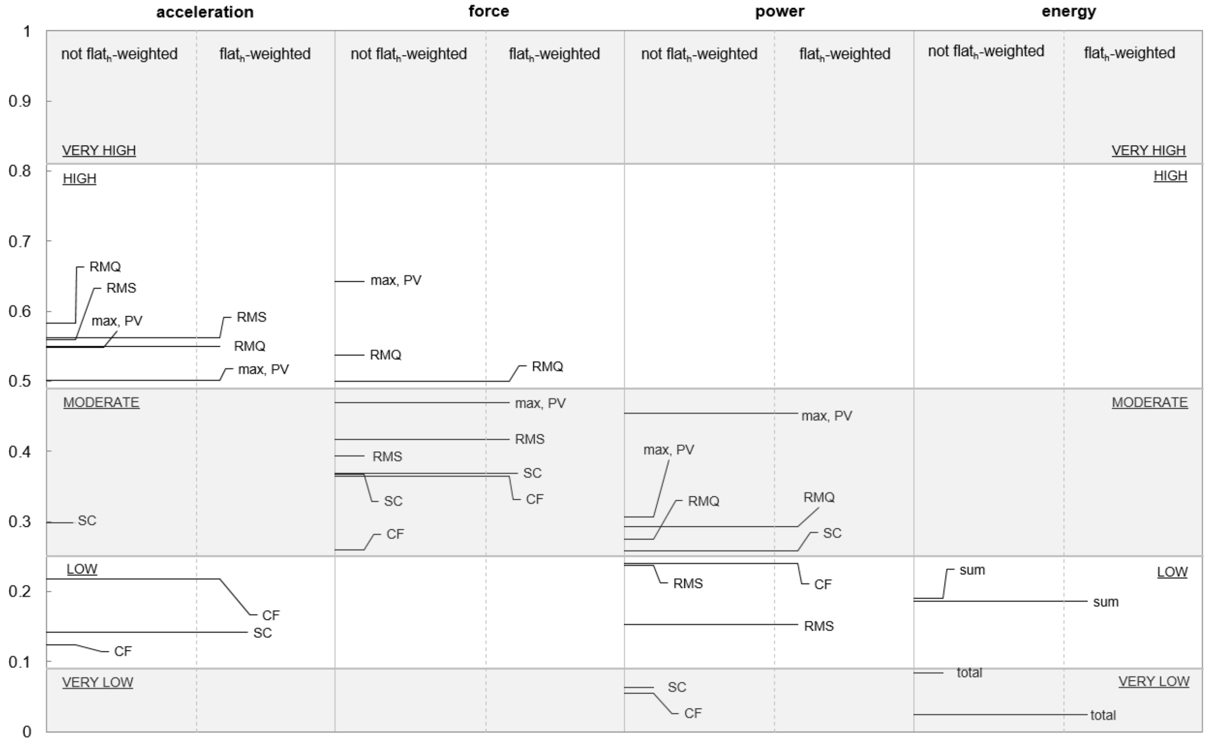

Fig. 9 The coefficient of determination between the DC force and each of the six derived parameters of the acceleration, force and power time signals and the energy integrals for each impact. Each value represents the mean of the left and right hand result (apart from the total energy). Note: PV: peak value; RMS: root mean square; RMQ: root mean quad; CF: crest factor; SC: shock content quotient; sum: integral sum of the energy. total: sum of the energy in left and right hands combined.

4.4 Final thoughts

More generally, we recommend that further work is conducted to investigate the effectiveness of the parameters assessed here under other test conditions. For example, it is the authors' recommendation that power or energy be investigated as metrics to (a) differentiate between the excitation levels of actual road surfaces, (b) assess differences in transmitted road-induced vibration through bicycles and bicycles components in isolation (e.g. frames with different vertical in-plane compliances, wheel geometries or tyres at different pressures), and (c) assess how effective they are when measured at the cyclist's buttocks instead of at the hands. The findings relating to the *PDR-DDR criterion* seem remarkable and have the potential to have importance in the context of RBDC research. Further work is suggested on this topic. It is the authors' opinion that the results for the acceleration-based parameters presented in this study should raise some concerns and should call for more investigation into their aptness for the study of RBDC, and this may also extend into the assessment of hand-arm vibration in general.

5 Conclusion

We aimed to determine the effectiveness of the four mechanical quantities commonly used to assess RBDC to discriminate between small changes in the level of an impact load applied at the front wheel of a road bicycle when measured at a cyclist's hands. Acceleration and force time signals were recorded at the left and right hands using instrumented brake hoods during a series of impacts at the front wheel on a bicycle treadmill. Six derived parameters of the acceleration, force and power time signals were considered: discrete values: maximum, peak; mean values: root mean square, root mean quad; ratio values: crest factor, shock content quotient. Integral values were used for the energy. A range of criteria were developed to assess the performance of these parameters and whether they should be recommended as RBDC metrics for impact events. The criteria were related to three characteristics: the consistency of the measurements, the parameter's statistical discrimination power, and how well changes in the parameter matched corresponding changes in impact level. The energy and root mean square value of power were found to be the top performers and are recommended as RBDC metrics for impact events. All acceleration-based parameters are not recommended. The remaining parameters demonstrated mixed results. Further investigative work is recommended to explore how effective these parameters are under other test conditions. Acceleration and force showed higher variability due to the cyclist's posture, whereas the highly recommended parameters were marginally influenced by the cyclists posture. We believe that the influence of the cyclist's posture should also be a topic for further study.

Conflict of interest The authors declare they have no conflict of interest.

References

1. Lépine J, Champoux Y, Drouet J-M (2015) The relative contribution of road bicycle components on vibration induced to the cyclist. Sports Eng 18:79-91
2. Ayachi F, Dorey S, Guastavino C (2015) Identifying factors of bicycle comfort: An online survey with enthusiast cyclists. Appl Erg 46:124–136
3. Vanwalleghem J, Mortier F, De Baere I, Loccufier M, Van Paepegem W (2012) Design of an instrumented bicycle for the evaluation of bicycle dynamics and its relation with the cyclist's comfort. Procedia Eng 34:485-490
4. Champoux Y, Vanwallenghem J, Drouet J-M (2015) Dynamic calibration of an instrumented bicycle brake hood in measuring power absorbed by the hands. Procedia Eng 112:225-230
5. Caya A, Champoux Y, Drouet J-M (2012) Dynamic behaviour and measurement accuracy of a bicycle brake hood force transducer. Procedia Eng 34:526–531
6. Vanwalleghem J, De Baere I, Loccufier M, Van Paepegem W (2015) Dynamic calibration of a strain gauge based handlebar force sensor for cycling purposes. Procedia Eng 112:219-224
7. Petrone N, Giubilato F (2013) Development of a test method for the comparative analysis of bicycle saddle vibration transmissibility. Procedia Eng 60:288-293
8. Thite AN, Gerguri S, Coleman F, Doody M, Fisher N (2013) Development of an experimental methodology to evaluate the influence of a bamboo frame on the bicycle ride comfort. Veh Syst Dyn 51:1287–1304
9. Lépine J, Champoux Y, Drouet J-M (2014) Road bike comfort: on the measurement of vibrations induced to cyclist. Sports Eng 17:113-122
10. Pelland-Leblanc J-P, Lepine J, Champoux Y, Drouet J-M (2014) Using power as a metric to quantify vibration transmitted to the cyclist. Procedia Eng 72:392-397
11. Lépine J, Champoux Y, Drouet J-M (2016) Test protocol for in-situ bicycle wheel dynamic comfort comparison, Procedia Eng 147:568-572
12. Lépine J, Champoux Y, Drouet J-M (2013) A laboratory excitation technique to test road bike vibration transmission. Exp Tech 40:227-234
13. Mason G, Larson M, Deng R, Reed D, Pahlmeyer M, Wright N, Wu Z, Yahata J (2016) A robust low cost device for measuring road induced vibrations. J Sci Cycling 5:13-17
14. Petrone N, Giubilato F (2011) Comparative analysis of wheels vibration transmissibility after full bicycle laboratory tests, 40° Convegno Nazionale AIAS, Palermo
15. Giubilato F, Petrone N (2012) A method for evaluating the vibrational response of racing bicycles wheels under road roughness excitation. Procedia Eng 34:409-414
16. Olieman M, Marin-Perianu R, Marin-Perianu M (2012) Measurement of dynamic comfort in cycling using wireless acceleration sensors. Procedia Eng 34:568-573
17. Pelland-Leblanc J-P, Lépine J, Champoux Y, Drouet J-M (2014) Effect of structural damping on vibrations transmitted to road cyclists. In: De Clerck J. (eds) Topics in Modal Analysis I, Volume 7. Conference Proceedings of the Society for Experimental Mechanics Series. Springer, Cham
18. Drouet J-M, Covill D, Duarte W (2018) On the exposure of hands to vibration in road cycling: an assessment of the effect of gloves and handlebar tape. Proceedings 2:213
19. Marcolin G, Paoli A, Panizzolo F A, Biasco G, Petrone N (2010) A method for the analysis of cyclist shorts with different pads for perineal area protection: comparison between drum and road tests. Procedia Eng 2:2831-2835
20. Hölzel C, Höchtl F, Senner V (2012) Cycling comfort on different road surfaces. Procedia Eng 34:479-484

21. Litzenberger S, Christensen T, Hofstätter O, Sabo A (2018) Prediction of road surface quality during cycling using smartphone accelerometer data. Proceedings 2:217
22. Taylor M D, Edgar A, Raine M (2018) Scottish cycling pavement assessment using hand–arm vibration exposure. Infrastructure Asset Management, pp 1-16
23. Bíl M, Andrášik R, Kubeček J (2015) How comfortable are your cycling tracks? A new method for objective bicycle vibration measurement. Transportation Research Part C: Emerging Technologies 56:415-425
24. Nuñez J Y M, Bisconsini D R, Rodrigues da Silva A N (2018) Combining environmental quality assessment of bicycle infrastructures with vertical acceleration measurements. Transportation Research Part A: Policy and Practice
25. Richard S, Champoux Y, Lépine J, Drouet J-M (2015) Using an alternative forced-choice method to study shock perception at cyclists' hands: the effect of tyre pressure. Procedia Eng 112:361-366
26. Drouet J-M, Guastavino C, Girard N (2016) Perceptual thresholds for shock-type excitation of the front wheel of a road bicycle at the cyclist's hands. Procedia Eng 147:724-729
27. Ayachi F S, Drouet J-M, Champoux Y, Guastavino C (2018) Perceptual thresholds for vibration transmitted to road cyclists. Human Factors 60:844–854
28. ISO/TS 15694:2004 Mechanical vibration and shock — Measurement and evaluation of single shocks transmitted from hand-held and hand-guided machines to the hand-arm system
29. Efron B, Tibshirani R J (1993) An Introduction to the Bootstrap. New York, NY: Chapman and Hall
30. Wood M (2005) Bootstrapped Confidence Intervals as an Approach to Statistical Inference. Organizational Research Methods 8:454-470
31. Gardner M J, Altman D (1986) Confidence intervals rather than P values: estimation rather than hypothesis testing. British Medical Journal (Clinical research ed.) 292:746-750
32. Lee D K (2016) Alternatives to P value: confidence interval and effect size. Korean journal of anesthesiology 69:555–562
33. Hinkle D E, Wiersma W, Jurs S G (2003) Applied Statistics for Behavioural Sciences. 5th Ed. Boston: Houghton Mifflin